

- 35 mM isoniazid, and 3.5 mM MnCl₂, buffered at pH 7.5 with 50 mM Hepes. Before InhA was added to the reaction mixture, it was stored in 1 mM EDTA, 1 mM dithiothreitol, and 0.5 mM phenylmethylsulfonyl fluoride, buffered at pH 7.5 with 50 mM Hepes. InhA activity was measured by removing aliquots from the incubation mixture and spectrophotometrically monitoring the turnover of fresh NADH to NAD⁺ at 340 nm in the presence of a fatty acyl-CoA substrate (6). InhA activity decreased by 90% within 2 days and coincided with the reaction mixture turning bright yellow. Crystals of isoniazid-inhibited InhA were produced by combining the incubation mixture in a 1:1 ratio with 12% methyl pentane diol, 4% dimethyl sulfoxide, 100 mM Hepes at pH 7.5, and 50 mM sodium citrate at pH 6.5, and placing it in a hanging drop enclosure. Within a week, crystals reached a size of 0.4 × 0.3 × 0.3 mm and were of the same morphology as those used previously to determine the native crystal structure (18).
20. A single crystal was used to collect a data set at room temperature with a MacScience DIP2030 image plate system with double-focusing mirrors coupled to a Rigaku x-ray generator, using a copper rotating anode with a 0.005-mm nickel filter and a 0.5-mm x-ray beam collimator. The Denzo and Scalepack package (26) was used to autoindex, integrate, and scale frames of data. Data collection statistics are listed in Table 1.
21. An initial difference Fourier ($F_o - F_c$) electron density map, in which the calculated phases were derived from the native InhA model with bound NADH (PDB 1eny), contained a single intense peak (7σ) with a size and shape distinctive of the isonicotinic acyl group derived from isoniazid. No other peaks existed in the map with the same intensity and characteristics. Refinement of the isoniazid-inhibited InhA model was performed with the X-PLOR software package (27) and a 2σ cutoff was applied to the structure factors, resulting in less than 2% of the data being omitted. Several rounds of manual model building and automated refinement with addition of the isonicotinic-acyl group and 68 ordered water molecules brought the R_{factor} to 20.2% and the R_{free} to 29.7% for data from 10.0 to 2.7 Å. Throughout this process, the validity of the model was confirmed by inspecting simulated annealing omit maps, in which either 10 contiguous residues or a 6 Å sphere was omitted. Model refinement statistics are listed in Table 1.
22. Before mass spectrometry, the isoniazid-inhibited InhA was separated from the other components of the reaction mixture (excess NADH, isoniazid, Mn²⁺ ions) by using a Pharmacia Superdex-75 HR-10/30 gel-filtration column equilibrated in 100 mM triethylammonium acetate, pH 7.0, at a flow rate of 0.5 ml/min. The fractions containing the isoniazid-inhibited InhA were pooled and concentrated to about 2 mg/ml. An enzymatic activity assay confirmed that the purified protein was inactive, which implies that the isonicotinic acyl-NADH was still bound to InhA. Portions of this enzyme preparation (10 to 20 μ l) were brought to 100 μ l with a solution of 50% methanol and 1% acetic acid in water. These dilutions were infused into a Finnigan LCQ electrospray mass spectrometer at 5 μ l/min. Spectra were analyzed in positive mode and averaged for 1 min. The mass value of 770 daltons obtained for the isonicotinic acyl-NADH, present within the isoniazid-inhibited InhA sample, corresponds to the addition of a mass fragment consisting of NADH with one hydrogen removed (mass = 664 daltons) plus a mass fragment consisting of an isonicotinic acyl group derived from isoniazid (mass = 106 daltons).
23. H. A. Shoeb *et al.*, *Antimicrob. Agents Chemother.* **27**, 399 (1985).
24. Reaction mixtures containing Mn²⁺ ions, [*ring*-¹⁴C]-isoniazid, and NADH (or NAD⁺) with and without InhA were applied to a Pharmacia Superdex-Peptide gel-filtration column and equilibrated in 50 mM Hepes, pH 7.5, at a flow rate of 0.5 ml/min. Each component of the starting mixture was separated and identified, and the radioactivity of each column fraction was measured in a scintillation counter. Incubations that lack InhA do not shift any portion of the radiolabel from the isoniazid peak to an area of the chromatogram of larger molecular mass near the NADH peak.
25. C. Baldock *et al.*, *Science* **274**, 2107 (1996).
26. Z. Otwinowski, in *Data Collection and Processing*, L. Sawyer, N. Isaacs, S. Bailey, Eds. [Science and Engineering Research Council (SERC), Daresbury Laboratory, Warrington, UK, 1993], pp. 56–62.
27. A. T. Brunger, *X-PLOR version 3.1, A System for X-Ray Crystallography and NMR* (Yale Univ. Press, New Haven, CT, 1992).
28. F. Paoletti *et al.*, *Chem.-Biol. Interactions* **76**, 3 (1990).
29. E. Lewin and J. G. Hirsh, *Am. Rev. Tuberc. Pulm. Dis.* **71**, 732 (1955); F. G. Winder and J. M. Denny, *Biochem. J.* **73**, 500 (1959); K. Ito *et al.*, *Biochemistry* **31**, 11606 (1992).
30. H. A. Shoeb *et al.*, *Antimicrob. Agents Chemother.* **27**, 404 (1985); H. A. Shoeb *et al.*, *ibid.*, p. 408; A. Hillar and P. C. Loewen, *Arch. Biochem. Biophys.* **323**, 438 (1995).
31. B. K. Sinha, *J. Biol. Chem.* **258**, 796 (1983).
32. Figure 1 was made with the program O, version 5.9 (T. A. Jones and M. Kjeldgaard, Uppsala University, Uppsala, Sweden). Figures 3 and 4 were made with Chemistry 4-D Draw (ChemInnovation Software, San Diego, CA), and Fig. 5 was made with INSIGHT II (Biosym Technologies, San Diego, CA).
33. Financial support was provided by the Welch Foundation and NIH grants GM-45859 and AI-36849. We thank C. Vilcheze and R. Bittman for supplying 2-trans-octenoyl-coenzymeA for InhA activity assays, M. W. Crankshaw for mass spectrometry analysis, members of the Center for Structural Biology at Texas A&M University (<http://reddrum.tamu.edu/vivek/Public>) for helpful discussions, and M. Edwards for manuscript preparation assistance. The coordinates have been deposited in the Protein Data Bank with entry number 1zid.

16 May 1997; accepted 4 November 1997

Ultraviolet-Induced Cell Death Blocked by a Selenoprotein from a Human Dermatotropic Poxvirus

Joanna L. Shisler, Tatiana G. Senkevich, Marla J. Berry, Bernard Moss*

Selenium, an essential trace element, is a component of prokaryotic and eukaryotic antioxidant proteins. A candidate selenoprotein homologous to glutathione peroxidase was deduced from the sequence of molluscum contagiosum, a poxvirus that causes persistent skin neoplasms in children and acquired immunodeficiency syndrome (AIDS) patients. Selenium was incorporated into this protein during biosynthesis, and a characteristic stem-loop structure near the end of the messenger RNA was required for alternative selenocysteine decoding of a potential UGA stop codon within the open reading frame. The selenoprotein protected human keratinocytes against cytotoxic effects of ultraviolet irradiation and hydrogen peroxide, providing a mechanism for a virus to defend itself against environmental stress.

The trace element selenium is essential for survival, as demonstrated by the early embryonic lethality of targeted disruption of the selenocysteine (Sec) tRNA gene (1). Several lines of evidence, mostly based on a decrease or increase in dietary selenium, suggest that selenoproteins have roles in antioxidant defenses, thyroid function, reproductive capacity, and protection against tumors and virus infections (2, 3). Although selenoproteins are present in Bacteria, Archaea, and Eukarya, heretofore no viral selenoprotein has been demonstrated. A recent analysis of the DNA sequence of molluscum contagiosum virus (MCV) revealed an open reading frame (ORF), MC066L, with homology to human glutathione peroxidase (4), a well-characterized selenoenzyme that reduc-

es cytotoxic peroxides (2, 5). The MCV contains more than 150 genes (6) and, like other poxviruses, replicates in the cytoplasm of infected cells (7). It resides exclusively in the human epidermis, where it causes persistent, benign neoplasms in children and essentially untreatable opportunistic infections in AIDS patients (8). Apoptosis plays an important role in the biology of the epidermis and may provide a mechanism for regression of some epidermal neoplasms (9). The putative MCV glutathione peroxidase may protect infected cells against ultraviolet (UV) irradiation, which is known to induce apoptosis through the action of hydrogen peroxide and superoxide anions (10).

The MC066L ORF was predicted to encode a selenoprotein because of the presence of a potential UGA stop codon, which could be decoded as Sec, within the region of homology with glutathione peroxidase (4). Recognition of the Sec codon is relatively inefficient and depends on a secondary structural selenocysteine insertion sequence (SECIS) element, which occurs immediately after UGA

J. L. Shisler, T. G. Senkevich, B. Moss, Laboratory of Viral Diseases, National Institute of Allergy and Infectious Diseases, National Institutes of Health, 4 Center Drive, MSC 0445, Bethesda, MD 20892-0445, USA.

M. J. Berry, Thyroid Division, Harvard Institutes of Medicine, 77 Avenue Louis Pasteur, Boston, MA 02115, USA.

*To whom correspondence should be addressed.

in prokaryotic mRNA and in the 3' noncoding region of eukaryotic mRNA (11). Inspection of the nucleotide sequence within and following the MC066L ORF suggested the presence of a SECIS element in the 3' noncoding region (Fig. 1) that would be required to read through the UGA codon for synthesis of the predicted 30-kD MC066L protein. Because the length of the MCV mRNA is not known, we constructed recombinant plasmids with a bacteriophage T7 promoter adjacent to the MC066L ORF with 2, 127, or 297 base pairs of downstream noncoding sequence (Fig. 1). DNA encoding an influenza virus hemagglutinin (HA) epitope tag of nine amino acids was added to the NH₂-terminus of the MC066L ORF to allow detection with monoclonal antibody (mAb) 12CA5 (12).

The plasmids containing the T7 promoter and MC066L ORF were transfected into BS-C-1 cells that were infected with recombinant vaccinia virus vTF7-3 encoding T7 RNA polymerase (13). A protein immunoblot revealed several nonspecific bands in all lanes and a 30-kD band specifically from cells transfected with plasmids that included both the MC066L ORF and the adjacent 127 (Fig. 2A, lane 4) or 297 (Fig. 2A, lane 5) nucleotides of MCV 3' noncoding sequence. The 30-kD band was not detected when the transfected plasmid contained the MC066L ORF without significant MCV 3' noncoding sequence (Fig. 2A, lane 3). The size of the protein was consistent with the length of the ORF, assuming translation of the UGA codon; the requirement for the 3' noncoding sequence confirmed the presence and 3' location of the predicted SECIS element. To bolster this interpretation, we made two MC066L plasmids with point mutations in the UGA codon. In one, the G at position 191 was changed to A, thereby converting UGA to a UAA stop codon that cannot be decoded as Sec (Fig. 1, MC066L-E). In the other plasmid, the G was changed to C, thereby converting the UGA to a serine codon, which should greatly enhance translation of the ORF (Fig. 1, MC066L-D). The infected and transfected cells were labeled with [³⁵S]methionine 7 to 16 hours after infection, and the proteins were immunoprecipitated with mAb 12CA5. Although there were background bands, a specific 30-kD polypeptide was prominent with the G→C mutation (Fig. 2B, lane 4), faint with the wild-type sequence (Fig. 2B, lane 3), and absent with the G→A mutation (Fig. 2B, lane 5).

Selenium incorporation was directly demonstrated by metabolically labeling infected and transfected cells with ⁷⁵Se (University of Missouri Research Reactor, Columbia, Missouri) and analyzing the lysates by gel electrophoresis. A single prominent 30-kD band was detected by autoradiography only when the transfections were performed with the

MC066L ORF containing 127 (Fig. 2C, lane 4) or 297 (Fig. 2C, lane 5) nucleotides of 3' noncoding sequence. The identity of the ⁷⁵Se-labeled 30-kD polypeptide was confirmed by immunoprecipitation with mAb 12CA5. The selenoprotein bands detected in uninfected cells (Fig. 2C, lane 1) were not seen in the infected and untransfected (Fig. 2C, lane 2) or other infected cells because the labeling was carried out after vaccinia virus shuts off the synthesis of cellular proteins. The absence of any labeled band in the infected and untransfected cells suggests that vaccinia virus, unlike MCV, does not encode a selenoprotein.

The putative SECIS element located about 40 nucleotides downstream of the MC066L ORF was initially identified by the presence of conserved nucleotides found in all eukaryotic SECIS elements (shown in bold in Fig. 3A) and by the characteristic

stem loop (14) [obtained by the manual manipulation of a structure derived from the FOLD program (15)]. The SECIS activity was confirmed by the functional substitution of MCV noncoding sequences for the SECIS element of type I iodothyronine deiodinase (16) (Fig. 3B). Thus, the 3' noncoding region following the MC066L ORF was necessary and sufficient for synthesis of homologous and heterologous selenoproteins.

Having established that MC066L encodes a selenoprotein, we investigated whether it could protect epithelial cells against UV- and hydrogen peroxide-induced cell death. Because vaccinia virus is cytotoxic, we cloned the MC066L ORF and 3' noncoding sequence, with or without the HA epitope tag, into a nonviral eukaryotic expression vector. Transfected HeLa cells were incubated with ⁷⁵Se, and lysates were analyzed by gel electrophoresis (17). Without the HA tag, a single

Fig. 1. Schematic of the recombinant forms of the MC066L ORF. Checkered bar, HA epitope tag sequence encoding the nonapeptide Tyr-Pro-Tyr-Asp-Val-Pro-Asp-Tyr-Ala derived from the influenza virus HA gene and recognized by mAb 12CA5 (BABC0); unfilled bar, MC066L ORF in frame with HA tag; gray bar, noncoding region between MC066L ORF and the adjacent ORF; black bar, SECIS element within noncoding region. First ATG, translation initiation codon at start of HA epitope tag; second ATG, original initiation codon of MC066L ORF; TGA, alternative Sec or stop codon; TAG, stop codon at end of MC066L ORF; TCA, serine codon derived by mutagenesis of Sec codon; TAA, stop codon derived by mutagenesis of Sec codon. Numbers: 1, the first nucleotide of the MC066L ORF; 190, the alternative Sec codon; 661, the MC066L stop codon; 960, the last nucleotide of the intergenic region between MC066L and MC065L. DNA segments were cloned between the Nco I and Bam HI restriction endonuclease sites of pMITeOlac.20/3, a plasmid closely related to pVOTE1 (28).

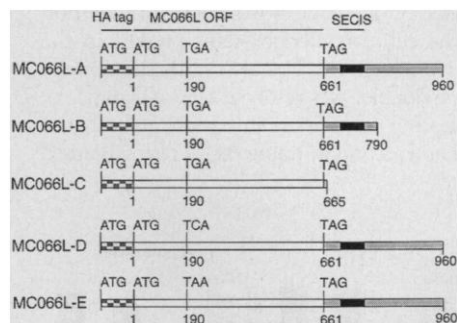


Fig. 2. Expression of MC066L ORF. **(A)** Protein immunoblots of MC066L protein. BS-C-1 cells, uninfected (lane 1) or infected with vTF7-3 (lanes 2 to 5), were transfected with no plasmid (lane 2) or MC066L-C (lane 3), MC066L-B (lane 4), or MC066L-A (lane 5). Abbreviations: 3'ncod, 3' noncoding region following MC066L ORF; T7 pol, T7 RNA polymerase. **(B)** SDS-PAGE autoradiograph of immunoprecipitated MC066L protein with point mutations. BS-C-1 cells, uninfected (lane 1) or infected with vTF7-3 (lanes 2 to 5), were transfected with no plasmid (lane 2) or with MC066L-A (lane 3), MC066L-D (lane 4), or MC066L-E (lane 5) and labeled with [³⁵S]methionine. **(C)** SDS-PAGE autoradiograph of ⁷⁵Se-labeled proteins. BS-C-1 cells, mock infected (lane 1) or infected with vTF7-3 (lanes 2 to 5), were transfected with no plasmid (lane 2) or with MC066L-C (lane 3), MC066L-B (lane 4), or MC066L-A (lane 5) and labeled with ⁷⁵Se. **(D)** SDS-PAGE autoradiograph of ⁷⁵Se-labeled proteins. HeLa cells, untransfected (lane 1) or transfected with the pCI vector (lane 2), the pCI vector containing the epitope-tagged MC066L-A (lane 3), or the untagged MC066L with 3'-noncoding sequences (lane 4), were labeled with ⁷⁵Se. Arrows: MC066L products.

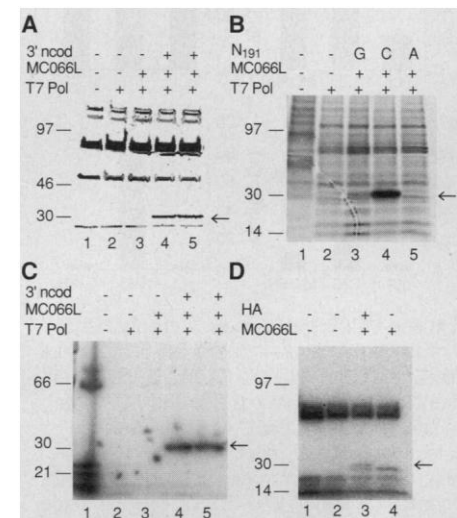
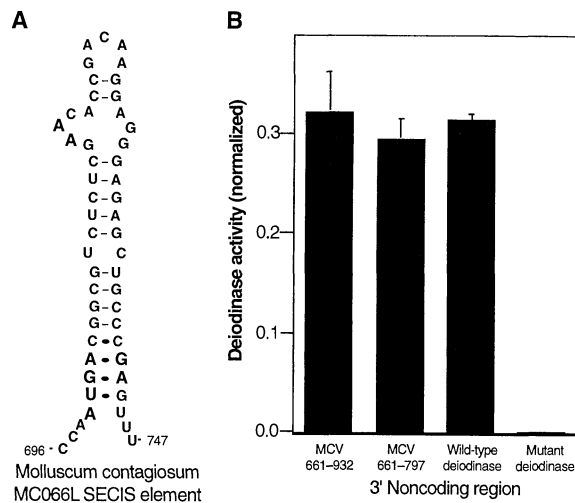


Fig. 3. Structure and function of MC066L SECIS element. **(A)** Predicted secondary structure. Nucleotides 696 and 747 correspond to the numbering system in Fig. 1, that is, the number of nucleotides from the start of the MC066 ORF. Invariant nucleotides present in all eukaryotic SECIS elements characterized to date are shown in bold. The filled oval symbols refer to predicted non-Watson-Crick base-pairing. **(B)** The MC066L SECIS element efficiently directs Sec incorporation into a heterologous cellular selenoprotein. Plasmids containing the rat type 1 deiodinase coding region followed by a DNA segment corresponding to MCV nucleotides 661 to 932 or 661 to 797 (Fig. 1) or the wild-type or mutant deiodinase SECIS element were transfected, together with a control plasmid that expresses human growth hormone, into human embryonic kidney 293 cells. Deiodinase activity, normalized to units of human growth hormone (16), of duplicate assays from two independent transfection experiments is shown.



labeled 30-kD band was detected in addition to the cellular selenoproteins present in the controls (Fig. 2D, lane 4). With the epitope tag, a doublet was resolved (Fig. 2D, lane 3), indicating translation initiation at both the first and second in-frame AUG codons caused

by nonoptimal sequences adjacent to the former. To evaluate a biological role of the MCV protein, we co-transfected cells with the MC066L vector (non-HA tag) and another plasmid that expresses the *Escherichia coli lacZ* gene. The pCI vector without the MC066L ORF or with the baculovirus P35 gene, a potent inhibitor of apoptosis (18), served as negative and positive controls, respectively. Transfected HeLa cells were irradiated with UV (Fig. 4A) or treated with hydrogen peroxide (Fig. 4B) and, after further incubation, were stained for β -galactosidase (β -Gal) and examined microscopically. Both UV irradiation and peroxide were found to induce cell rounding, membrane blebbing, and lifting of cells off the plate. Transfected cells were identified by their blue color, and the percentage that appeared flat and without signs of apoptosis was determined (19). The viability was higher when cells were transfected with MC066 or P35, compared to vector alone, indicating that the proteins encoded by these genes were protective. The ability of P35 to protect against UV-induced apoptosis was previously reported (19, 20).

Similar protective effects of the transfected genes were also obtained with a spontaneously immortalized human keratinocyte cell line, HaCaT (21), which undergoes apoptosis when UV-irradiated (22). Cells transfected with vector alone were more sensitive to UV irradiation (Fig. 4C) and hydrogen peroxide (Fig. 4D) than those expressing MC066L or P35. Unlike P35, MC066L did not protect HeLa cells from cytotoxicity induced by tumor necrosis factor (TNF) (Fig. 4E) or by antibody to Fas (anti-Fas) (Fig. 4F), suggesting that the activity of the MCV protein is restricted to blocking UV- and peroxide-induced signals.

The protein encoded by MC066L is the

only documented example of a virus-encoded selenoprotein. The absence of homologs of this gene in vaccinia (23) and variola (24) viruses suggest that the glutathione peroxidase was acquired by MCV after the divergence of the *Molluscipoxvirus* and *Orthopoxvirus* genera from a common progenitor, or that it was lost from the latter at about that time. A relatively recent acquisition of MC066L is supported by the 75% amino acid identity with human glutathione peroxidase, a value considerably higher than the values of 20 to 25% for other MCV proteins with cellular homologs (6). In addition, the sequence following the MC066L gene contains a functional eukaryotic SECIS element, as demonstrated by its ability to substitute for the element of a heterologous cellular selenoprotein.

Viruses have evolved a number of ways of preventing or delaying cell death so as to increase the yield of progeny (25). MCV was recently shown to encode two genes with death effector domains, and at least one of these can prevent TNF- and anti-Fas-mediated cytolysis (19, 26). These MCV genes could complement MC066L because our data suggest that MC066L does not prevent TNF- or anti-Fas-mediated apoptosis. It is not presently possible to evaluate the in vivo roles of MCV genes because the virus does not replicate in tissue culture and replicates only minimally in animal models, precluding either the generation or testing of deletion mutants (27). Nevertheless, the ability of the MC066L gene to protect cells against UV- and peroxide-induced cell death is consistent with the enzymatic properties of glutathione peroxidases (2, 5) and would seem to be a clever ploy for a virus that replicates exclusively in the epidermis.

REFERENCES AND NOTES

1. M. R. Bsl, K. Takaku, M. Oshima, S. Nishimura, M. M. Taketo, *Proc. Natl. Acad. Sci. U.S.A.* **94**, 5531 (1997).
2. C. Michiels, M. Raes, O. Toussaint, J. Remacle, *Free Radical Biol. Med.* **17**, 235 (1994).
3. B. J. Lee, S. I. Park, J. M. Park, H. S. Chittum, D. L. Hatfield, *Mol. Cells* **6**, 509 (1996).
4. T. G. Senkevich *et al.*, *Science* **273**, 813 (1996).
5. T. C. Stadtman, *Annu. Rev. Biochem.* **65**, 83 (1996).
6. T. G. Senkevich, E. V. Koonin, J. J. Bugert, G. Darai, B. Moss, *Virology* **233**, 19 (1997).
7. C. D. Porter, N. W. Blake, J. J. Cream, L. C. Archard, *Mol. Cell. Biol. Hum. Dis. Ser.* **1**, 233 (1992).
8. S. L. Gottlieb and P. L. Myskowski, *Int. J. Dermatol.* **33**, 453 (1994).
9. A. R. Haake and R. R. Polakowska, *J. Invest. Dermatol.* **101**, 107 (1993).
10. A. Gorman, A. McGowan, T. G. Cotter, *FEBS Lett.* **404**, 27 (1997).
11. S. C. Low and M. J. Berry, *Trends Biochem. Sci.* **21**, 203 (1996).
12. J. Field *et al.*, *Mol. Cell. Biol.* **8**, 2159 (1988).
13. The BS-C-1 cells were infected with vTF7-3 and transfected as described [T. R. Fuerst, E. G. Niles, F. W. Studier, B. Moss, *Proc. Natl. Acad. Sci. U.S.A.* **83**, 8122 (1986)] except for the use of lipofectin (Life Technologies). After 16 hours, the cells were lysed and analyzed by SDS-polyacrylamide gel electro-

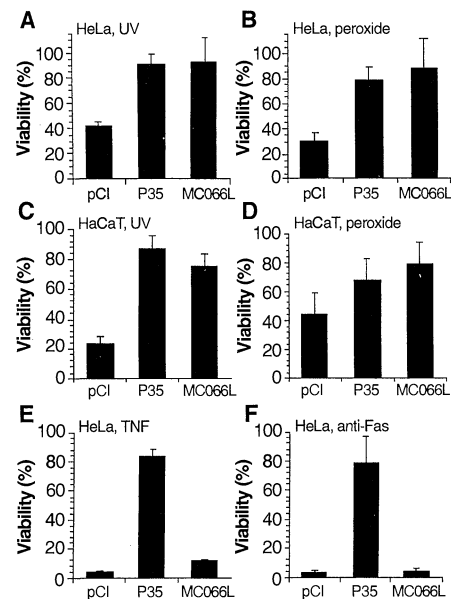


Fig. 4. The MC066L protein protects against UV- and hydrogen peroxide-induced cell death. HeLa **(A, B, E, and F)** or HaCaT **(C and D)** cells were co-transfected with CMV- β -Gal and pCI vector, pCI-P35, or pCI-MC066L-A. Thirty hours after transfection, the cells were UV irradiated **(A and C)** or were treated with hydrogen peroxide **(B and D)**, cycloheximide and TNF- α **(E)**, or cycloheximide and anti-Fas **(F)**. After 12 additional hours, the cells were fixed and stained with X-Gal, and the percent viability of the blue cells was determined. The data shown are the means and standard errors of three separate transfection experiments.

Change in Chemoattractant Responsiveness of Developing Axons at an Intermediate Target

Ryuichi Shirasaki,* Ryuta Katsumata, Fujio Murakami

Developing axons reach their final targets as a result of a series of axonal projections to successive intermediate targets. Long-range chemoattraction by intermediate targets plays a key role in this process. Growing axons, however, do not stall at the intermediate targets, where the chemoattractant concentration is expected to be maximal. Commissural axons in the metencephalon, initially attracted by a chemoattractant released from the floor plate, were shown to lose responsiveness to the chemoattractant when they crossed the floor plate in vitro. Such changes in axon responsiveness to chemoattractants may enable developing axons to continue to navigate toward their final destinations.

In the developing nervous system, axons navigate considerable distances toward their final targets in a highly stereotyped and directed manner. This process is achieved by a series of axonal projections to successive intermediate targets under the influence of local guidance cues (1). Accumulating evidence has indicated the importance of long-range chemoattraction in guiding developing axons not only to final (2) but also to intermediate targets (3–10). Commissural axons originating from the alar plate of the vertebrate central nervous system, for example, initially grow ventrally, attracted by a diffusible chemotropic molecule secreted from the ventral midline floor plate (3–9), an intermediate target of these axons (6, 11). These axons, however, grow past the floor plate to extend contralaterally. Since the first demonstration of the existence of the floor plate–derived chemoattractant (3), an intriguing question has been why growing axons do not stall at their intermediate targets, where the chemoattractant concentration is expected to be maximal. Here, we provide evidence for a change in the chemoattractant responsiveness of growing axons during their growth across an intermediate target.

Metencephalon commissural axons, which originate from the cerebellar plate (CP) of the rat embryo, initially grow circumferentially toward floor plate cells at the ventral midline of the metencephalon (6). In vitro studies have suggested that these commissural axons (referred to hereafter as CP axons) are guided toward the midline by a diffusible chemoattractant released from floor plate cells (6, 7, 9). Here, we used an in vitro preparation that reproduces the crossing of the midline floor plate by CP axons to examine possible changes in the chemoattractant responsiveness of CP axons when they cross the floor plate (12). When a strip of the rostral metencephalon

that included the entire circumferential trajectory of CP axons (Fig. 1A) was cultured alone in collagen gel, axons originating from the CP grew across the midline floor plate to extend contralaterally ($n = 16$) (Fig. 1B) (13). We next tested whether CP axons, after they have crossed the floor plate, are attracted by an ectopic floor plate explant. We juxtaposed a floor plate explant to the metencephalic strip on one side (Fig. 1A) and examined the behavior of CP axons by implanting the fluorescent tracer 1,1'-dioctadecyl-3,3,3',3'-tetramethylindocarbocyanine perchlorate (DiI) into the CP contralateral to the explant. Under such conditions, CP axons that had crossed the midline floor plate did not show directed growth toward the ectopic floor plate explant (Fig. 1C). To compare directly the behavior of CP axons extending from both sides, we implanted DiI crystals into the contralateral CP and 3,3'-dioctadecyloxycarbocyanine perchlorate (DiO) crystals into the ipsilateral CP of the same strip preparations (Fig. 1D). Although DiO-labeled CP axons that had not crossed the midline floor plate showed directed growth toward the ectopic explant, DiI-labeled axons that had crossed showed no sign of directed growth (Fig. 1, D and E).

Because implantation of DiI or DiO into the CP might also label axonal populations other than those from commissural neurons, such as longitudinally growing axons (Fig. 1C) (6), we next assessed chemoattraction of CP axons by labeling them with a molecular marker for commissural axons (14). Commissural axons at all axial levels from the spinal cord to the mesencephalon express TAG-1, an axonal surface glycoprotein, during their circumferential growth until they reach the floor plate in vivo (9, 15). Moreover, TAG-1–positive (TAG-1⁺) commissural axons including CP axons are attracted by the floor plate in vitro (3, 9). We found that most TAG-1⁺ CP axons in control strip preparations grew straight along the circumferential axis ($n = 15$) (Fig. 1F), although some TAG-1⁺ CP axons near the cut edges of the prep-

- phoresis (SDS-PAGE). The proteins were transferred to a polyvinylidene difluoride membrane (Millipore) and incubated with mAb 12CA5 (BABCO, Richmond, CA) followed by an alkaline phosphatase–conjugated antibody to murine immunoglobulin G (Promega). Membranes were developed using a stabilized substrate for alkaline phosphatase (Promega).
14. R. Walczak, E. Westhof, P. Carbon, A. Krol, *RNA* **2**, 367 (1996).
 15. M. Zuker and P. Stiegler, *Nucleic Acids Res.* **9**, 133 (1981).
 16. The DNA segment corresponding to nucleotides 661 to 932 or 661 to 797 (Fig. 1) as subcloned downstream of the rat type 1 deiodinase coding region in the mammalian expression vector pUHD10 [M. Gossen and H. Bujard, *Proc. Natl. Acad. Sci. U.S.A.* **89**, 5547 (1992)]. Plasmids containing the wild-type deiodinase SEClS element or a nonfunctional mutant of this element downstream of the deiodinase coding region served as positive and negative controls, respectively. The plasmids with deiodinase sequences were transfected, together with a control plasmid that expresses human growth hormone, into human embryonic kidney 293 cells. Deiodinase activity, in counts per minute of iodine released per microliter of transfected cell sonicate, was normalized to units of human growth hormone in 100 μ l of medium, as described [G. W. Martin III, J. W. Harney, M. J. Berry, *RNA* **2**, 171 (1996)].
 17. Transfection procedures: HeLa cells were co-transfected with 1 μ g of cytomegalovirus (CMV)- β -Gal (Stratagene) and 5 μ g of pCI vector (Promega), pCI-P35 (18), or pCI-MC066L-A mixed with lipofectin. Thirty hours after transfection, the cells were treated with UV (312 nm) light for 15 s at room temperature or continuously with 100 μ M hydrogen peroxide or cycloheximide (1 μ g/ml; Sigma) and TNF- α (10 ng/ml; Boehringer Mannheim) or cycloheximide and anti-Fas (1.25 μ g/ml; CH-11 antibody, Kamiya Biomedical, Seattle, WA). Twelve hours later, cells were fixed, stained with X-Gal (Promega), and examined microscopically. The control wells contained 100 to 200 flat, blue cells per microscopic field. The number of flat, blue cells in six fields of the untreated well of each transfectant was compared to the number of flat, blue cells in six fields of the treated well, and the percent viability was determined. The HaCat cells were co-transfected with 0.33 μ g of CMV- β -Gal and 1.67 μ g of pCI, pCI-P35, or pCI-MC066L-A mixed with lipofectamine reagent (Life Technologies). Thirty hours after transfection, the cells were treated for 30 s with UV (312 nm) light or 10 μ M hydrogen peroxide. Cells were fixed, stained, and scored for viability as described for HeLa cells.
 18. R. J. Clem and L. K. Miller, *Mol. Cell. Biol.* **14**, 5212 (1994).
 19. J. Bertin *et al.*, *Proc. Natl. Acad. Sci. U.S.A.* **94**, 1172 (1997).
 20. G. A. Manji, R. R. Hozak, D. J. LaCount, P. D. Friesen, *J. Virol.* **71**, 4509 (1997).
 21. P. Boukamp, R. T. Petrussevska, J. Hornung, A. Markham, N. E. Fusenig, *J. Cell Biol.* **106**, 761 (1988).
 22. U. Henseleit, T. Rosenbach, G. Kolde, *Arch. Dermatol. Res.* **288**, 676 (1996).
 23. S. J. Goebel *et al.*, *Virology* **179**, 247 (1990).
 24. R. F. Massung *et al.*, *ibid.* **201**, 215 (1994).
 25. J. G. Teodoro and P. E. Branton, *J. Virol.* **71**, 1739 (1997).
 26. M. Thome *et al.*, *Nature* **386**, 517 (1997); S. Hu, C. Vincenz, M. Buller, V. M. Dixit, *J. Biol. Chem.* **272**, 9621 (1997).
 27. R. M. L. Buller, J. B. W. Chen, J. Kreider, *Virology* **213**, 655 (1995); K. H. Fife *et al.*, *ibid.* **226**, 95 (1996).
 28. G. A. Ward, C. K. Stover, B. Moss, T. R. Fuerst, *Proc. Natl. Acad. Sci. U.S.A.* **92**, 6773 (1995).
 29. We thank D. Hatfield for suggestions regarding selenium labeling of proteins and J. Bertin and J. Cohen for critically reading the manuscript, providing pCI-P35, and offering advice regarding transfections and viability assays. Supported in part by NIH grant DK47320 (M.J.B.).

Laboratory of Neuroscience, Division of Biophysical Engineering, Graduate School of Engineering Science, Osaka University, Toyonaka, Osaka 560, Japan.

*To whom correspondence should be addressed. E-mail: shirasaki@bpe.es.osaka-u.ac.jp

3 September 1997; accepted 28 October 1997